The Mu2e experiment: STM Detector.

Claudia Alvarez Garcia.
claudia.alvarezgarcia@postgrad.manchester.ac.uk

Motivation.


NEWS

Home | Coronavirus | Brexit | UK | World | Business | Politics | Tech | Science | Health | Family & Education

Science & Environment

Muons: 'Strong' evidence found for a new force of nature

By Pallab Ghosh
Science correspondent

7 April

REIDAR HAHN / FERMILAB

The findings come from the US Muon g-2 experiment

Hints from FNAL Muon g-2 and LHCb that muons may not be behaving as we expect in the Standard Model.

New physics explaining these anomalies could also cause a charged lepton flavour violating (CLFV) transition in muons.

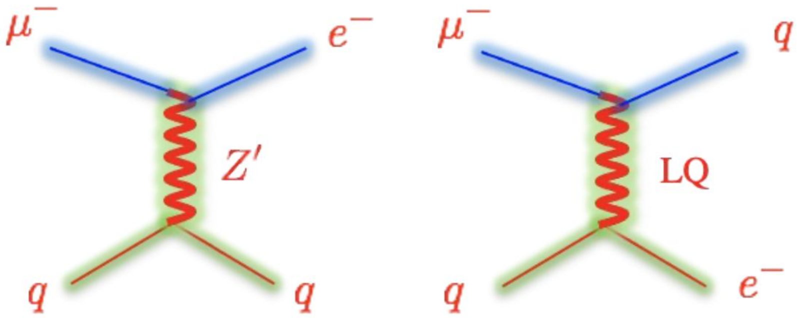

CLFV only occurs in SM via neutrino oscillations over tiny distance : it is thus heavily suppressed to 10^{-50} level.

Thus **ANY** observation of CLFV would be evidence of new physics.

Muon cLFV and origin of Neutrino Masses.

cLFV observables can provide information on the New Physics model.

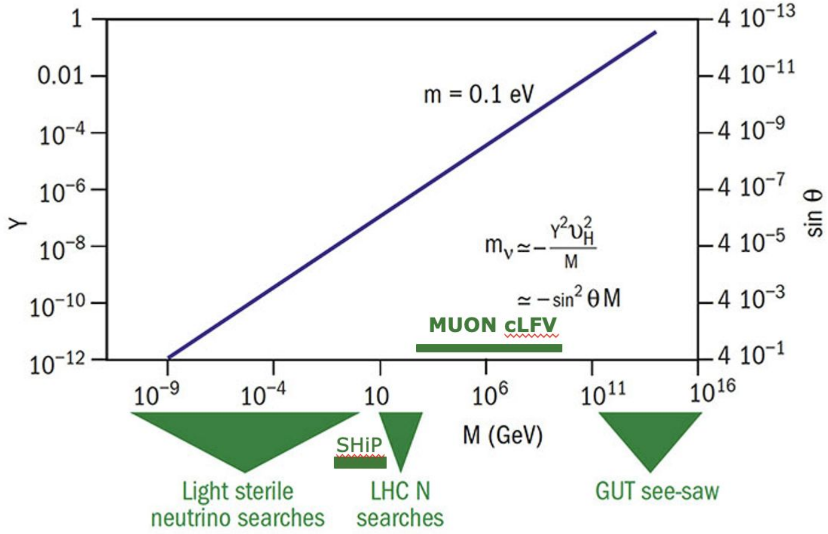

Very wide range in possible RH neutrino masses.

- In the minimal extended SM: neutrino oscillations (masses) are intimately connected with charged lepton flavour violation.

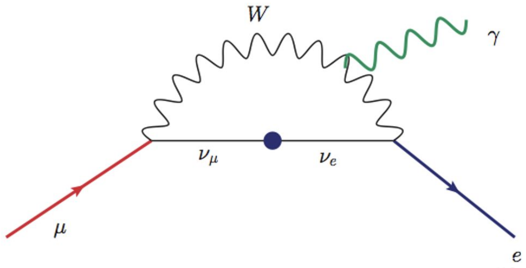

$$BR_{SM+neutrino\,masses}(\mu^- \to e^-) < 10^{-50}$$

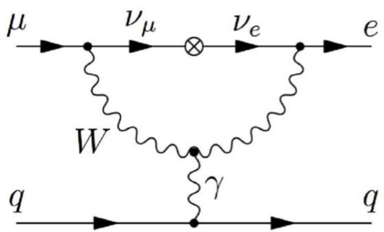

$$\mu^- N \to e^- N$$

Although the BR is strongly suppressed.

- In BSM extensions to the Higgs sector also predict cLFV:

$$\nu_{RH} \to l^- H^+$$

The Mu2e Experiment.

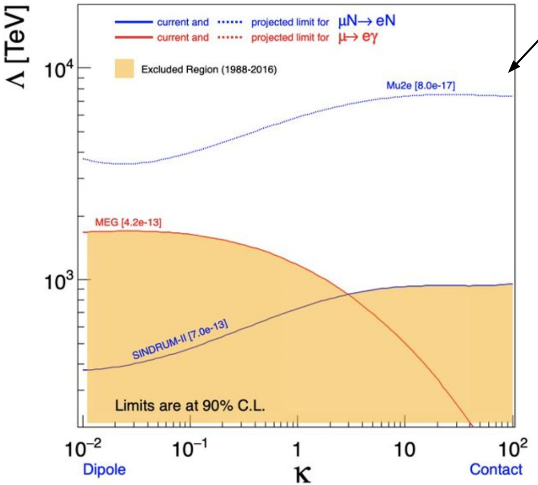

Updated from A. de Gouvea, P. Vogel, arXiv:1303.4097

Mu2e experiment can probe both dipole and contact BSM interactions to mass scales in the multi-TeV region

Muon is captured by aluminium and forms a muonic atom and in doing so it emits characteristic X-rays

As a muonic atom:

- Muon can decay as usual emitting e- and neutrinos
- Be captured by nucleus
- Signal: **Undergo CLFV and emit e- (conversion electron: CE) and NO neutrinos**

Main Background: Muon Decay in Orbit (DIO)

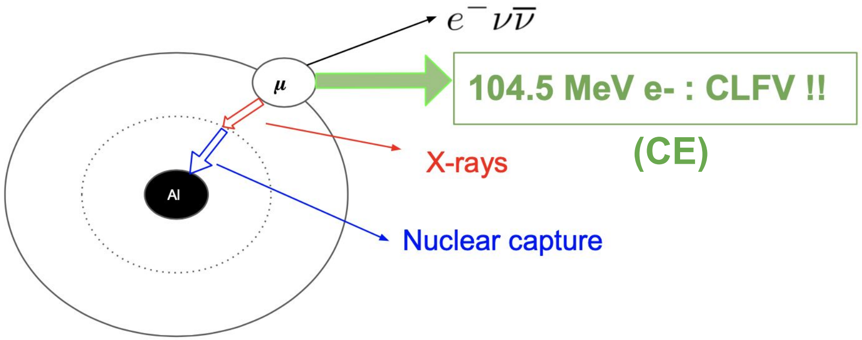

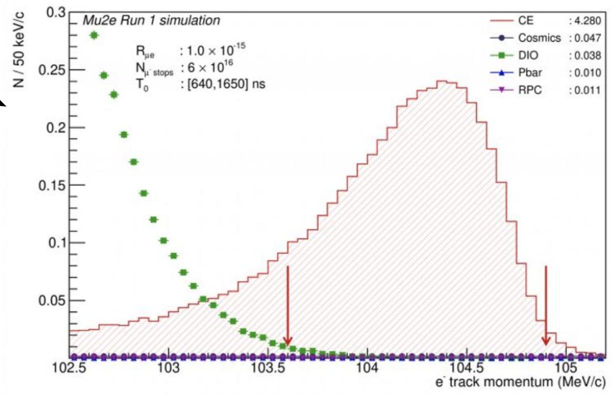

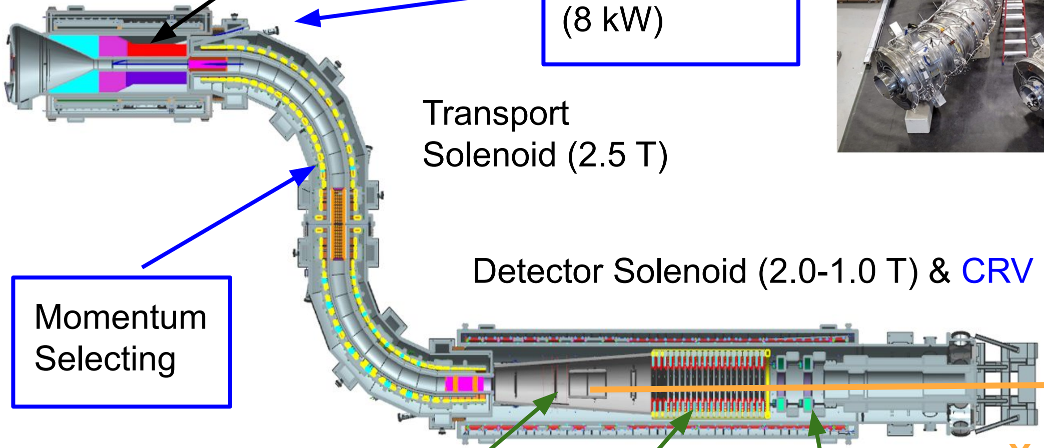

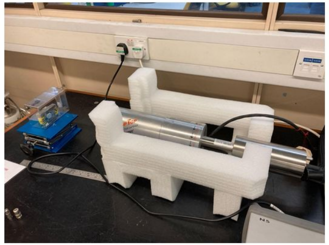

STM Detector:
HPGe and LaBr

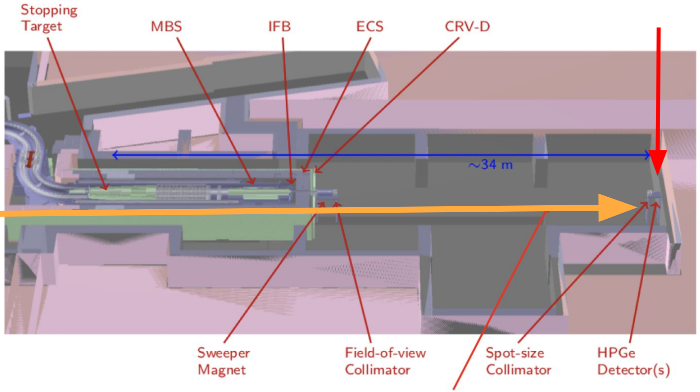

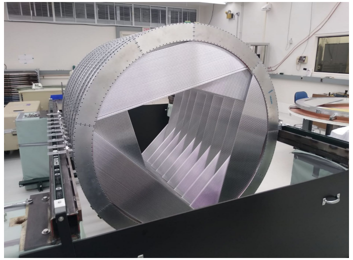

35 m

Sensitivity of 8×10^{-17} requires 10^{10} muons/s to interact with the aluminium (stopping) target.

Muons (< 75 MeV/c) are captured by the aluminium and in that process characteristic X-rays are emitted.

We detect these X-rays 35m away from the target to “count the muons”.

STM: HPGe detector.

From: CaenElectronicInstrumentation

ADC: signed 16-bit values

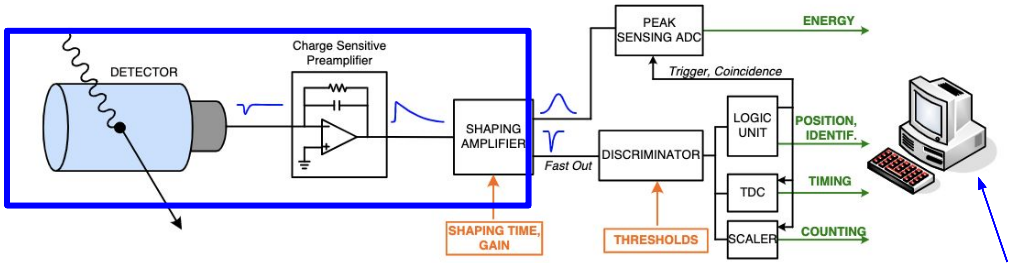

Analysis: Pulse Finding

HPGe

FPGA: Field Programmable Gate Array

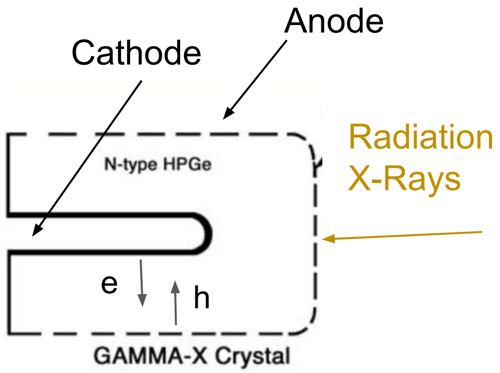

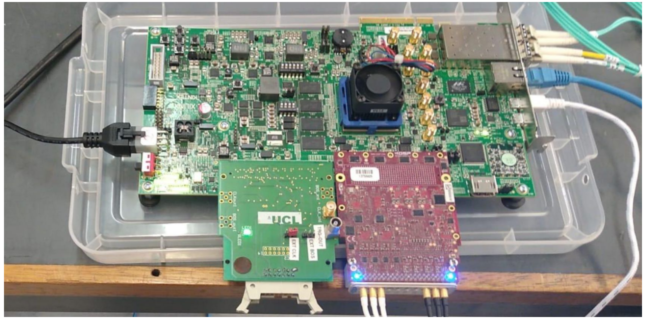

FMC-ADC: Two channels for Ge and two channels for HPGe

Both HPGe and LABr detectors detect these X-rays via a collimated aperture with a line of sight to the Al-target.

I am working with the HPGe detector: the DAQ, calibration, simulation and optimisation of this detector.

Developing pulse finding algorithms that can run at MHz rates to determine X-ray energy and identify characteristic peaks.

- ADC Counts range from (−32768, +32767) and it's equal to a range voltage of -0.85 - 0.85 V peak to peak.

Taken data with: Co-60, Cs-137 and Eu-152 sources at Liverpool
ADC is -0.85V to +0.85V. Sampling here at 360 Ms/sec (2.78 ns). 16 bit precision.

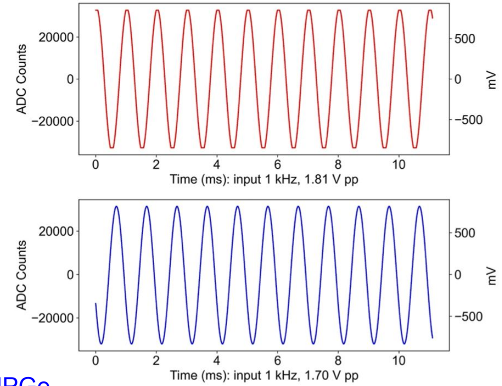

Zero Suppression Algorithm.

- Store just data with peaks: removing noise.
- There are many possible zero suppression algorithms - any we develop must be implementable in VHDL.
- Input: 2 parameters:
    - ADC threshold (ADC_T)
    - Window time (W_T)

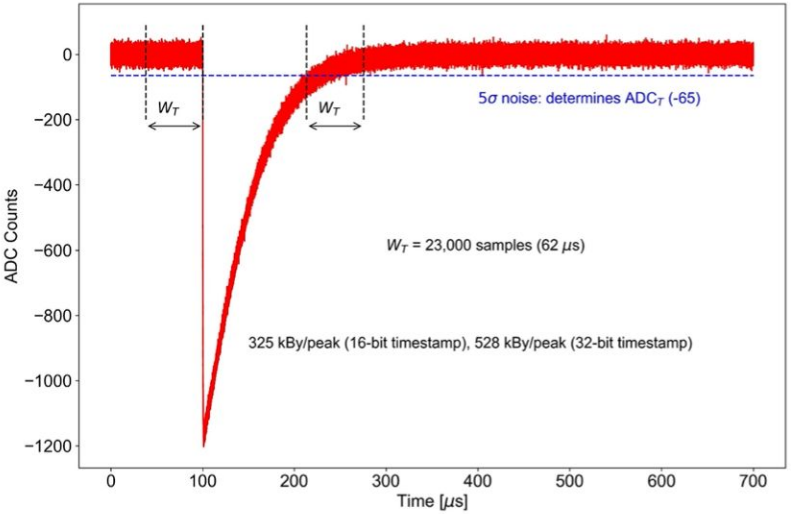

- Example as first approach: C++ (assuming we know the baseline and the RMS).

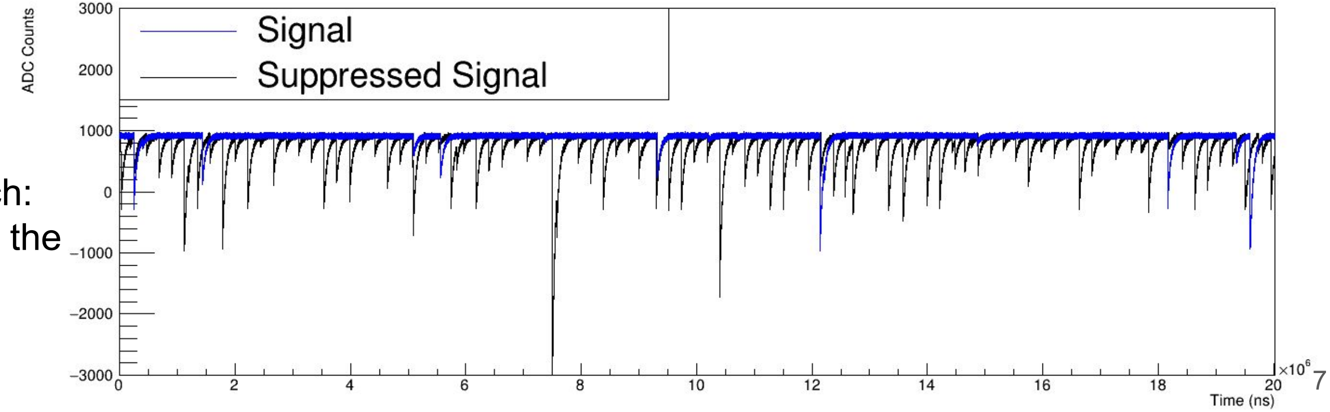

MWD + Pulse Finding Algorithm.

- Signal.
- Deconvolution:

$$A[i] = V[i] - \left(1 - \frac{T_0}{\tau_{decay}}\right) V[i-1] + A[i-1]$$

- Differentiation:

$$D[i] = A[i] - A[i-M]$$

- Averaging:

$$l[i] = \frac{1}{L} \sum_{k=i-L}^{i-1} D[k]$$

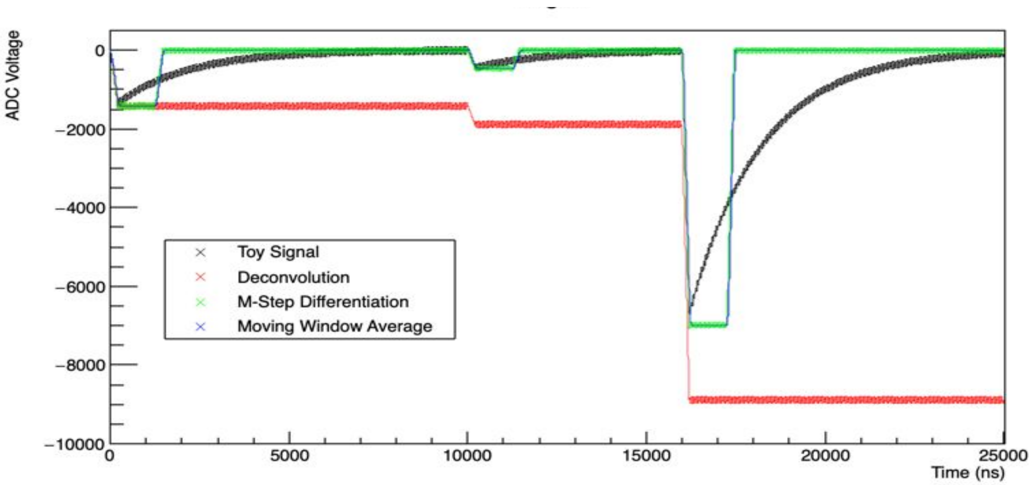

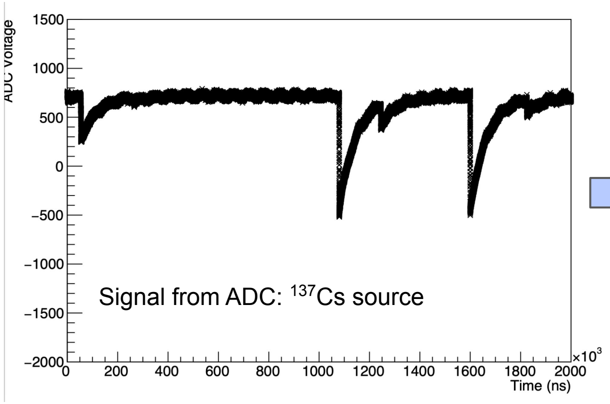

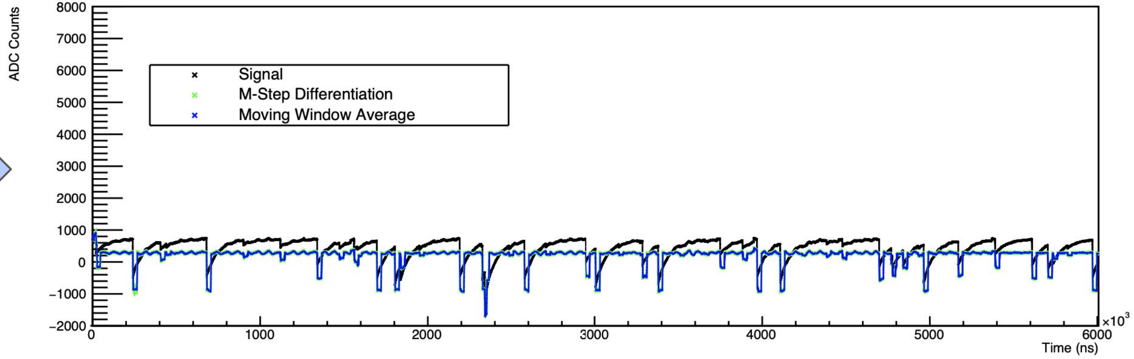

Computing time and input parameters.

- DAQ: midas file.
  - midas to csv
  - midas to binary

File	Size	Bytes	Time Reading the file
.CSV	669 Mb	$278 \cdot 10^6$	1:30.79 total
.BIN	266 Mb	$278 \cdot 10^6$	15.516 total

Computing time is improved by a factor of: ∼6 using binary files.

- Input parameters MWD.
  - M, L parameters.
  - ADC runs at 370 MHz, so T_0= 2.7 ns, τ=55748.2 ns.

- Input parameters Pulse Finding: Baseline of ADC counts.
- Result: process 7.59 ns/ADC value, 505 peaks found per sec.

Sample Size	Read data	MWD + peak finder time	time/ADC value (per CPU-core)	Number of peaks found
536870912 ADC values	325 milliseconds	4114 milliseconds	7.66 ns	2244

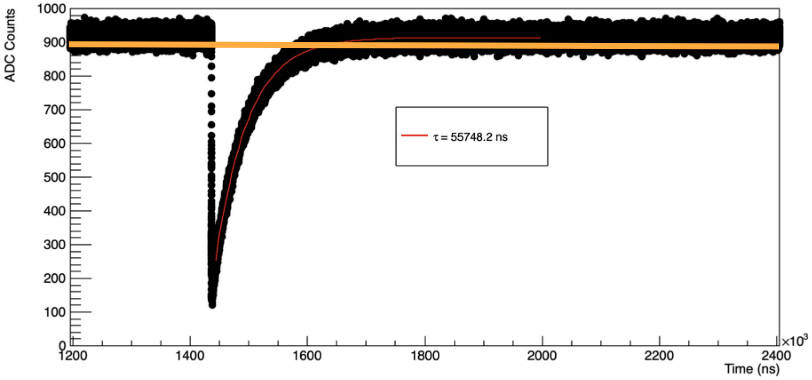

^{137}Cs and ^{152}Eu source: ADC-Energy Calibration.

MWD + Pulse Finding

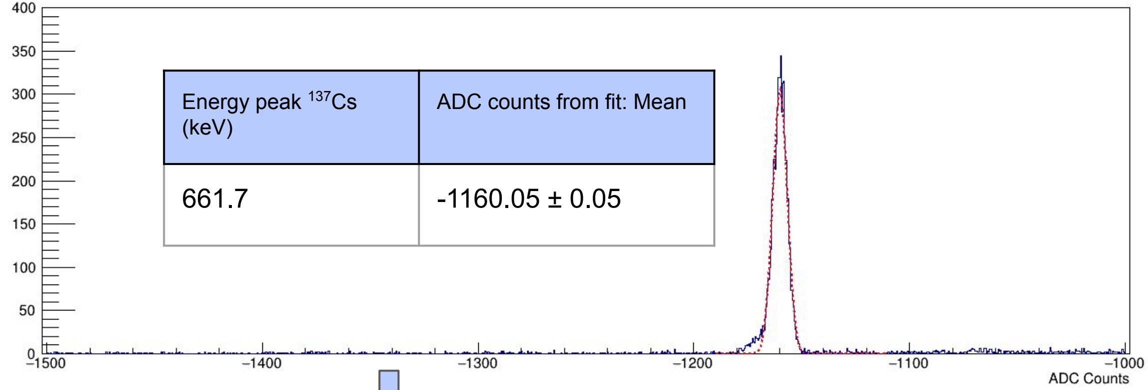

Energy peak ^{137}Cs (keV)	ADC counts from fit: Mean
661.7	-1160.05 ± 0.05

^{137}Cs

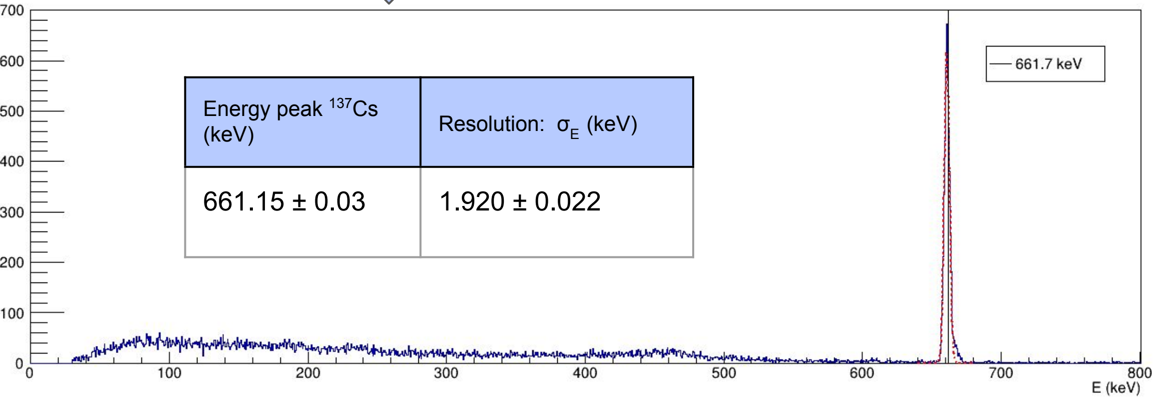

Energy peak ^{137}Cs (keV)	Resolution: σ_E (keV)
661.15 ± 0.03	1.920 ± 0.022

^{137}Cs + ^{152}Eu Calibration

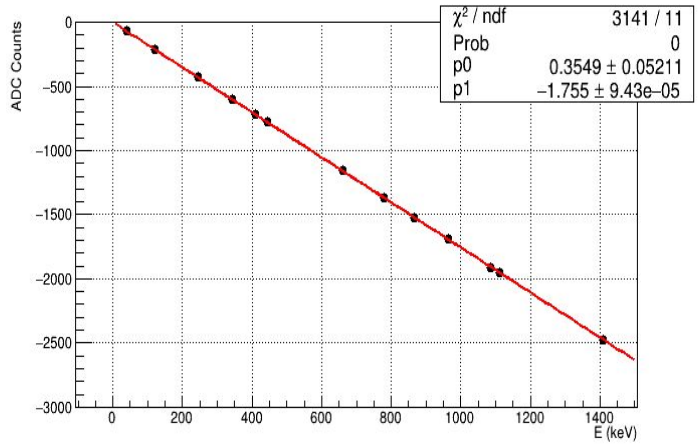

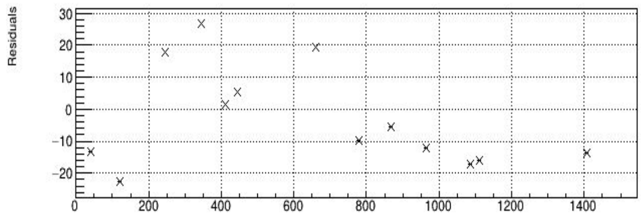

$$ADC = -1.755 \cdot E\,(keV) + 0.3549$$

$$1\,ADC = \frac{1}{1.755\,keV} = 0.57\,keV$$

Results.

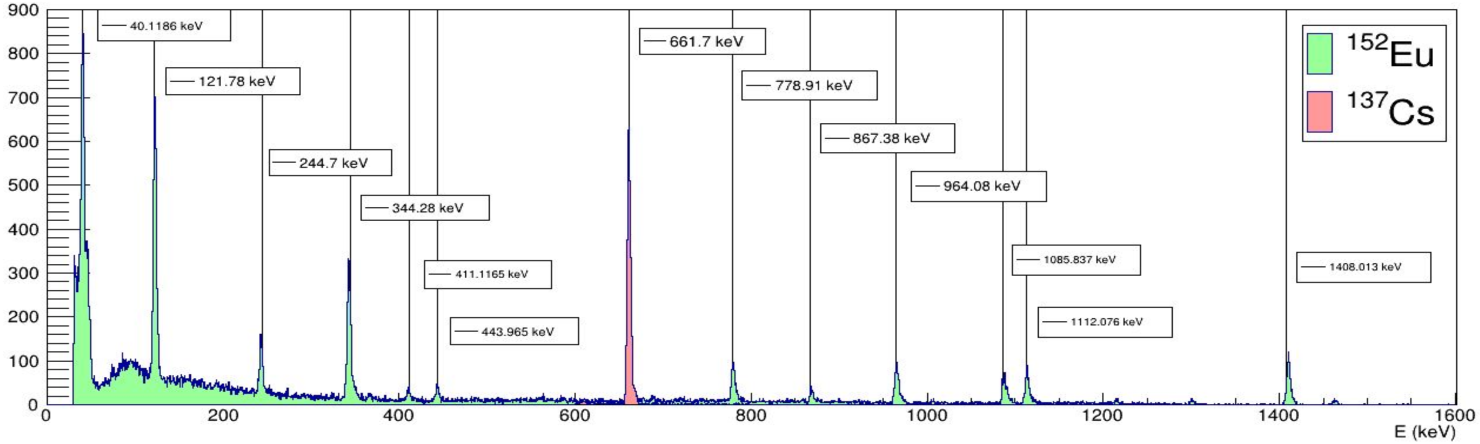

Resolutions (σ not FWHM) depend on the run: 1.6 - 2.3 keV at 662 keV (^{137}Cs peak).

Here we have assumed a linear ADC to E calibration : it is **NOT.**

Expect efficiency to decrease with energy.

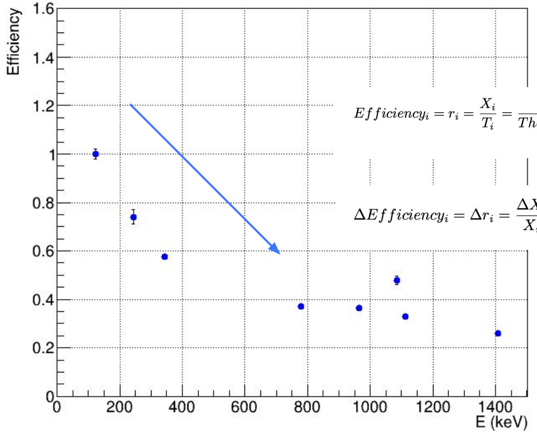

^{152}Eu

$$Efficiency_i = r_i = \frac{X_i}{T_i} = \frac{Ncounts[peak_i]/N_{REF}[121keV]}{TheoryRate[peak_i]/TheoryRate[121keV]}$$

$$\Delta Efficiency_i = \Delta r_i = \frac{\Delta X_i}{X_i} r_i = r_i \sqrt{\frac{1}{Ncounts[peak_i]} + \frac{1}{N_{REF}}}$$

Resolution analysis from data.

- ADC resolution: σ_{ADC}= 0.57 keV.

$$Error\,\Delta\left(\frac{\sigma_{TOT}}{E_{reco}}\right) = \frac{\sigma_{TOT}}{E_{reco}}\sqrt{\left(\frac{\Delta\sigma_{TOT}}{\sigma_{TOT}}\right)^2 + \left(\frac{\Delta E_{reco}}{E_{reco}}\right)^2}$$

- HPGe resolution from ORTEC: σ_{HPGe} (1330 keV) ≈ 1 keV.

- Detector resolution: $\sigma^2_{Detector} = \sigma^2_{TOT} = \sigma^2_{HPGe} + \sigma^2_{ADC}$

Having into account just the variation in the number of electron-hole pairs generated as a result of ionization statistics

- Assuming: $\sigma_{HPGe} = k_E \sqrt{E} \Rightarrow \sigma_{HPGe}$ (1330 keV) ≈ 1keV=$k_E \sqrt{1330}$ keV ⇒ k_E = 0.027 $keV^{1/2}$

  σ_{HPGe} (662 keV) ≈ 0.7 keV

- Detector + ADC resolution is: $\sigma_{Detector}$ (662 keV) = 0.9 keV

- Algorithm resolution 1.6 - 2.1 keV.
- From results: it is clear that we have other contributions to the HPGe resolution.

  $\sigma^2_{HPGe} = (k_E \sqrt{E})^2 + C^2$

- C accounts for uncertainties introduced by: Detector noise + Charge collection efficiency and Algorithm (MWD optimised parameters…).

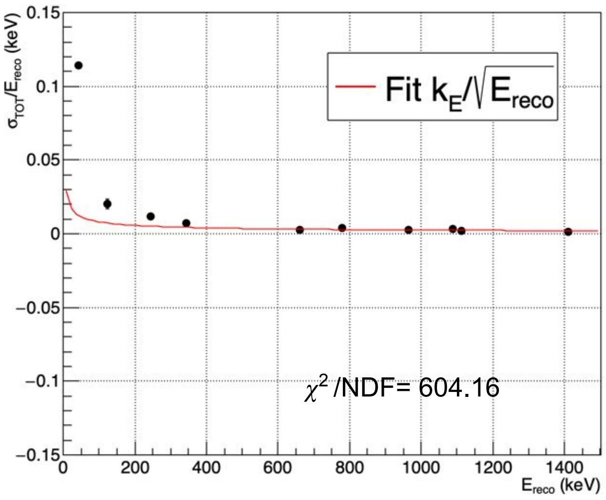

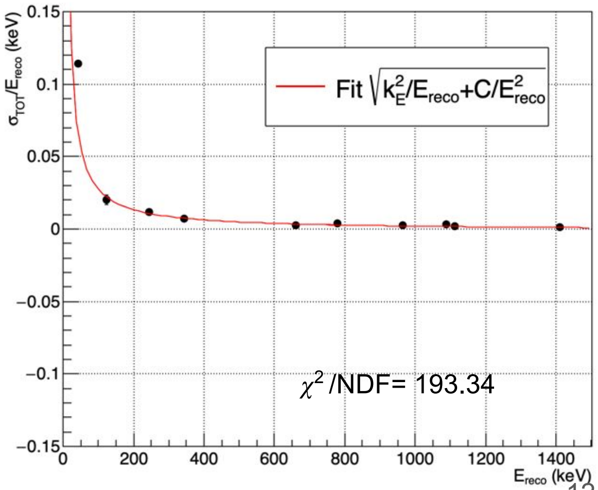

HPGe Energy Resolution: Theoretical Analysis.

$$\sigma_{HPGe} \neq \sigma_E$$

$$\sigma^2_{HPGe} = \sigma^2_{electronic\,noise} + \sigma^2_{charge\,collection} + \sigma^2_E$$

Noise caused by the detector leakage current and the preamplifier. It's independent of E_γ

Variation in the ability to detect the number of e-h pairs created by the ionization process: e-h pairs that recombine before they can be collected, or charge carriers that fall into traps while drifting to their respective electrode

Variation in the number of e-h pairs created due to ionization statistics.

$$\sigma_E = k_E\sqrt{E_{reco}}$$

$$k_E = \sqrt{F\epsilon_{eh}}$$

The Fano Factor: *F, statistics in the number of e-h pairs created*

- F =0: Absolutely deterministic conversion of energy into e-h pairs. No fluctuations in the number of e-h pairs created.
- F =1: Completely independent random ionization events. No correlation between the number of e-h pairs created and the phonons produced, Poisson's statistics apply.

From data to Geant4 Simulation.

Example of the variation of the FWHM of the full-energy peak of an 86 cm^3 HPGe detector with gamma-ray energy.
From: RadiationDetectionAndMeasurementbyKnoll

$$\frac{\sigma_{TOT}}{E} = \sqrt{\frac{\sigma^2_{charge\,collection} + \sigma^2_E + \sigma^2_{electronic\,noise} + \sigma^2_{ADC}}{E^2}} = \sqrt{\frac{DE^2 + k_E^2 E + C}{E^2}} = \sqrt{D + \frac{k_E^2}{E} + \frac{C}{E^2}}$$

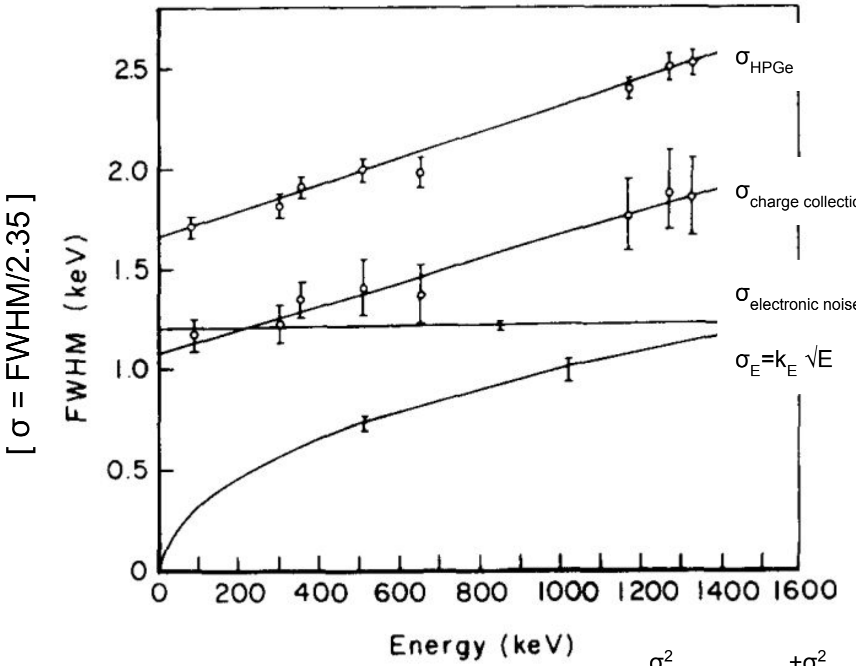

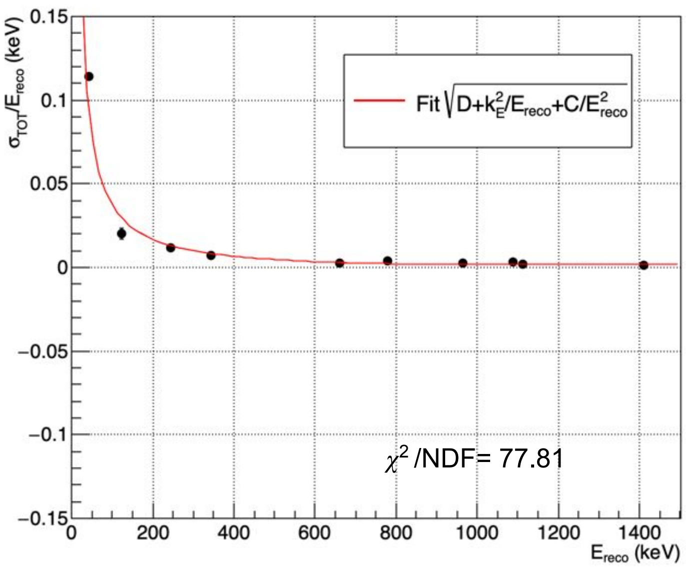

k_E, Fano Factor ? ⇒ Geant4 Simulation

HPGe Resolution.

Germanium properties:

$$E_{bindingenergy}(\mathrm{Ge}) = 11.103\,\mathrm{keV}$$

$$\epsilon_{eh}(\mathrm{Ge}) = 2.97\,\mathrm{eV}$$

Main processes causing energy depositions:

- Photoelectric Effect. $E_{e-} = E_\gamma - E_{bindingenergy}$ → Maximum energy deposited in the photopeak
- Compton Effect. $E_{\gamma'} = \dfrac{2E_\gamma mc^2}{2mc^2 + 2E_\gamma(1 - cos\theta)}$ → Compton Background

  $E_{e-'} = 1 - E_{\gamma'}$
- Pair Production. $E_\gamma > 1.022$ MeV

Resolution: Energy deposited +

Creation of electron-hole (e^--h) pairs.

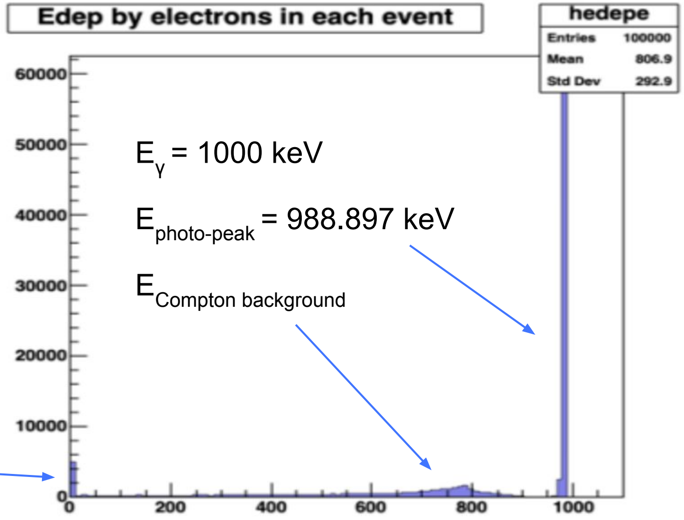

Leave the detector without interacting

Geant4: Rate Photoelectric to Compton effect.

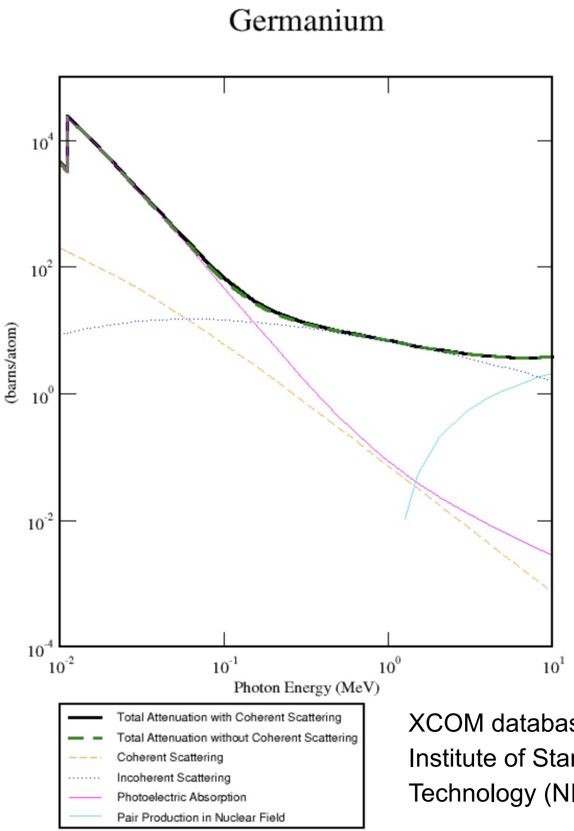

XCOM database. National Institute of Standards and Technology (NIST)

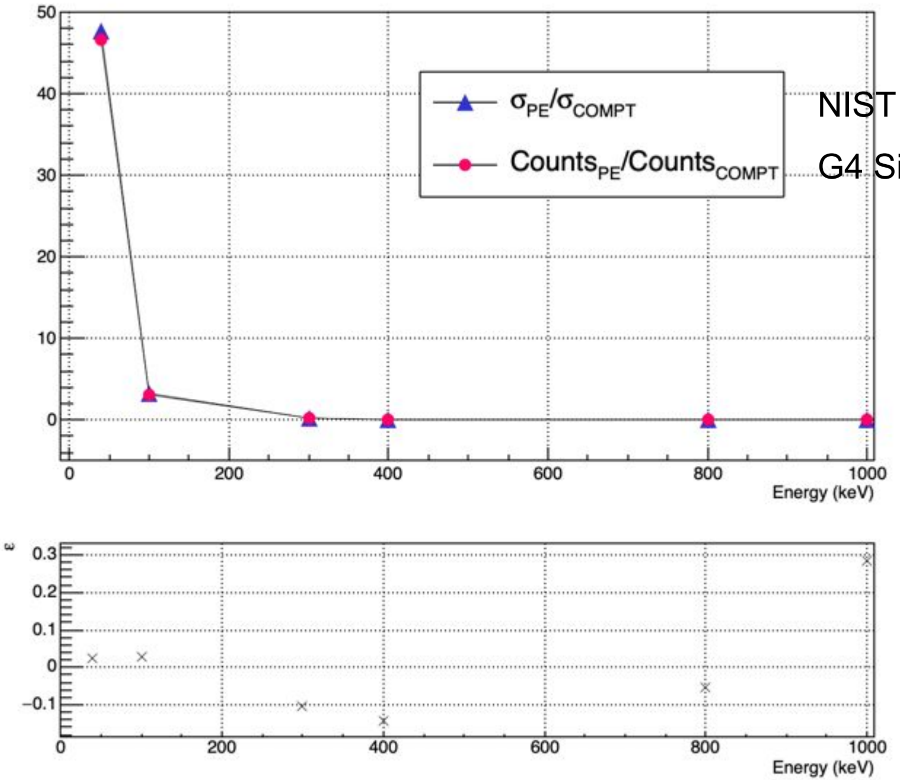

NIST

G4 Simulation

Geant4: Creation and Sampling of e⁻-h pairs.

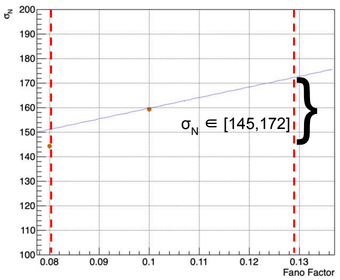

Creation of eh pairs

$$N_{e-h}true = \frac{edepstep(eV) - NIEL}{2.97eV}$$

$NIEL$=Non Ionizing Energy Loss

Table 11.1 Properties of Intrinsic Silicon and Germanium

	Si	Ge
Atomic number	14	32
Atomic weight	28.09	72.60
Stable isotope mass numbers	28-29-30	70-72-73-74-76
Density (300 K); g/cm^3	2.33	5.32
Atoms/cm^3	4.96×10^{22}	4.41×10^{22}
Dielectric constant (relative to vacuum)	12	16
Forbidden energy gap (300 K); eV	1.115	0.665
Forbidden energy gap (0 K); eV	1.165	0.746
Intrinsic carrier density (300 K); cm^{-3}	1.5×10^{10}	2.4×10^{13}
Intrinsic resistivity (300 K); $\Omega \cdot$ cm	2.3×10^5	47
Electron mobility (300 K); cm^2/V · s	1350	3900
Hole mobility (300 K); cm^2/V · s	480	1900
Electron mobility (77 K); cm^2/V · s	2.1×10^4	3.6×10^4
Hole mobility (77 K); cm^2/V · s	1.1×10^4	4.2×10^4
Energy per electron–hole pair (300 K); eV	3.62	
Energy per electron–hole pair (77 K); eV	3.76	2.96
Fano factor (77 K)	0.143 (Ref. 7)	0.129 (Ref. 9)
	0.084 (Ref. 8)	0.08 (Ref. 10)
	0.085 to 0.137 (Ref. 12)	< 0.11 (Ref. 11)
		0.057 – 0.064 (Ref. 12)
	0.16 (Ref. 13)	0.058 (Ref. 14)

Source: G. Bertolini and A. Coche (eds.), *Semiconductor Detectors*, Elsevier-North Holland, Amsterdam, 1968, except where noted.

Sampling eh pairs: Gamma function

$$N_{e-h}reco = f(x|\alpha,\beta) = \frac{\beta^{\alpha}x^{\alpha-1}e^{-\beta x}}{\Gamma(\alpha)}$$

$$\alpha = N_{e-h}true \cdot \frac{1}{F}$$

$$\beta = \frac{1}{F}$$

$$F = Fano\,Factor, F(\mathrm{Ge}) = 0.10 \pm 0.02$$

For germanium

$$k_E = \sqrt{F\epsilon_{eh}} = \sqrt{0.1 \cdot 0.00297keV} = 0.017keV^{\frac{1}{2}}$$

662 keV photons

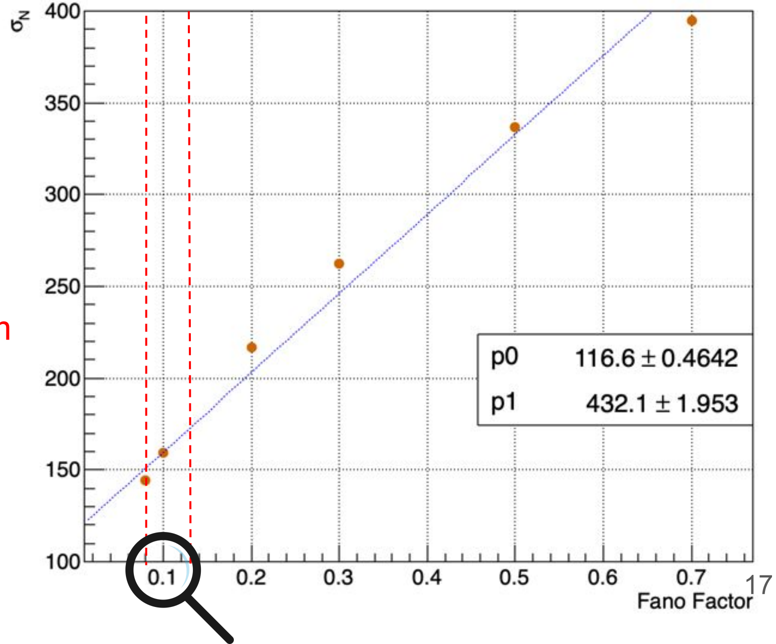

Geant4: HPGe Resolution in N_{eh} pairs.

Generated   After sampling with Gamma Function. *F*=0.1

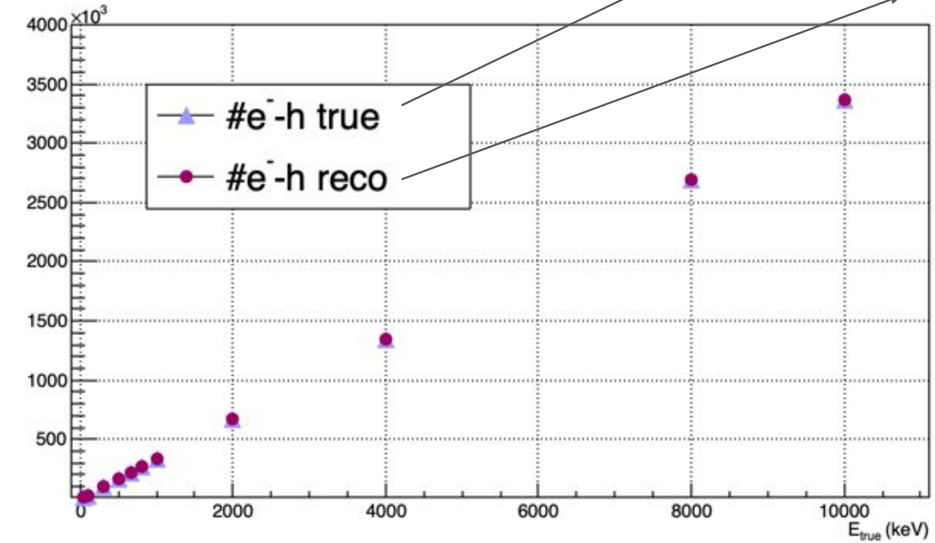

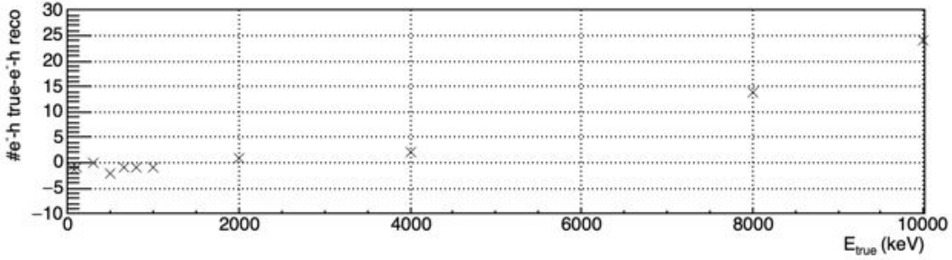

- Resolution in N_{eh} pairs:

$$FWHM_N = 2.35\sqrt{NF}$$

$$\sigma_N = \sqrt{\frac{E_{reco}}{\epsilon_{eh}}F} = k_N\sqrt{E_{reco}}$$

For germanium:

$$k_N = 5.80 \pm 0.23\, keV^{-\frac{1}{2}}$$

- The resolution of an HPGe is commonly expressed as:

$$\Delta E_{E_{carrier\ statistics}} = R \cdot E_{reco} = 2.35\sqrt{F\epsilon_{eh}E_{reco}}$$

N_{eh} Resolution.

$$\frac{\sigma_N}{E_{reco}} = k_N \cdot \frac{1}{\sqrt{E_{reco}}}$$

$$Error\ \Delta\left(\frac{\sigma_N}{E_{reco}}\right) = \frac{\sigma_N}{E_{reco}}\sqrt{\left(\frac{\Delta\sigma_N}{\sigma_N}\right)^2 + \left(\frac{\Delta E_{reco}}{E_{reco}}\right)^2}$$

$$\sigma_N = \sqrt{\frac{E_{reco}}{\epsilon_{eh}}F} = k_N\sqrt{E_{reco}}$$

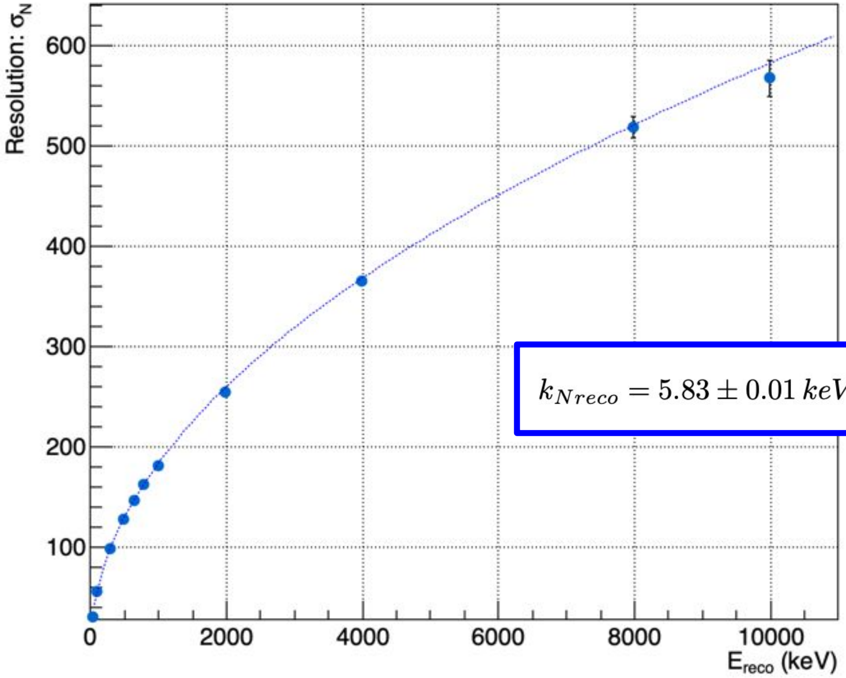

$$k_{Nreco} = 5.83 \pm 0.01\, keV^{-\frac{1}{2}}$$

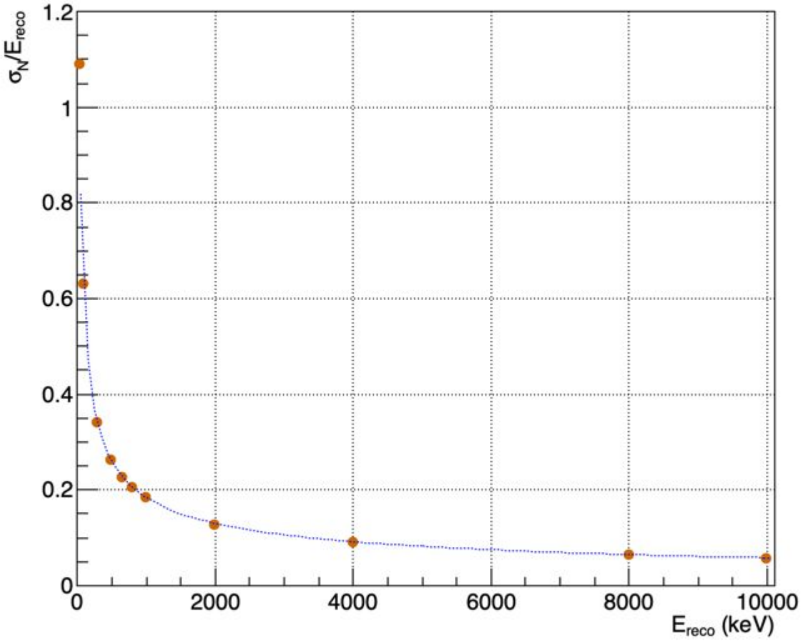

Result in good agreement with the one provided by the theory: $k_N = 5.80 \pm 0.23\, keV^{-\frac{1}{2}}$

Efficiency.

$$Eff = \frac{number\ of\ eh\ pairs\ in\ the\ photopeak}{number\ of\ gamma\ rays\ emitted\ from\ a\ source}$$

Expected tendency for GEM Detector.

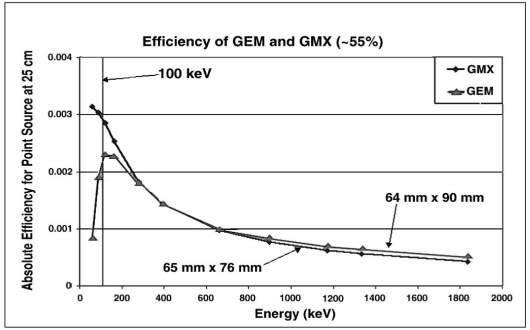

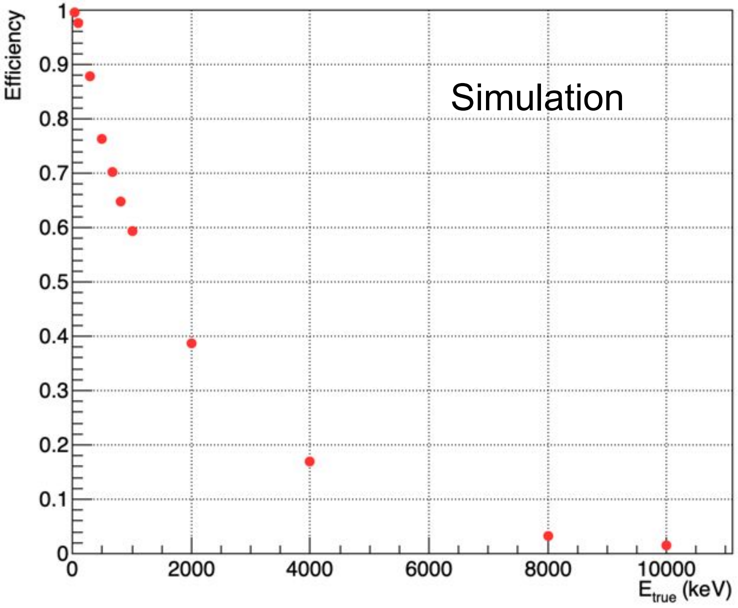

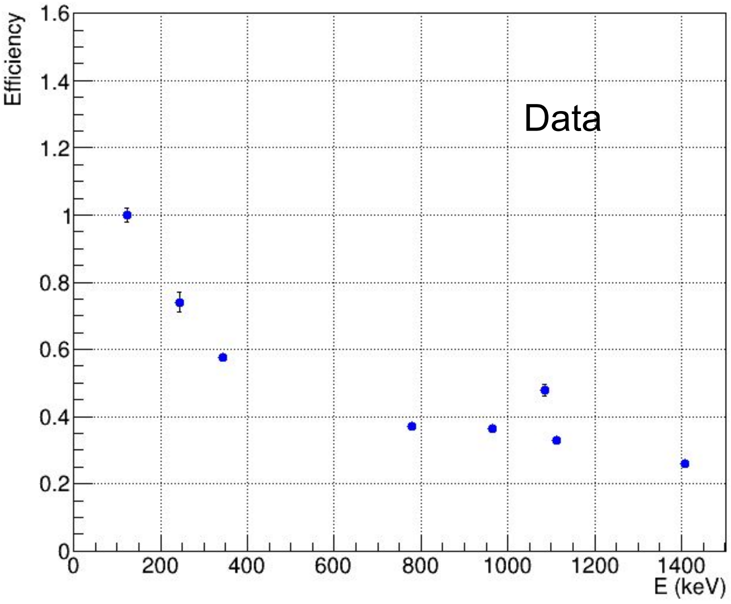

The STM in ART: Testing the Geometry.

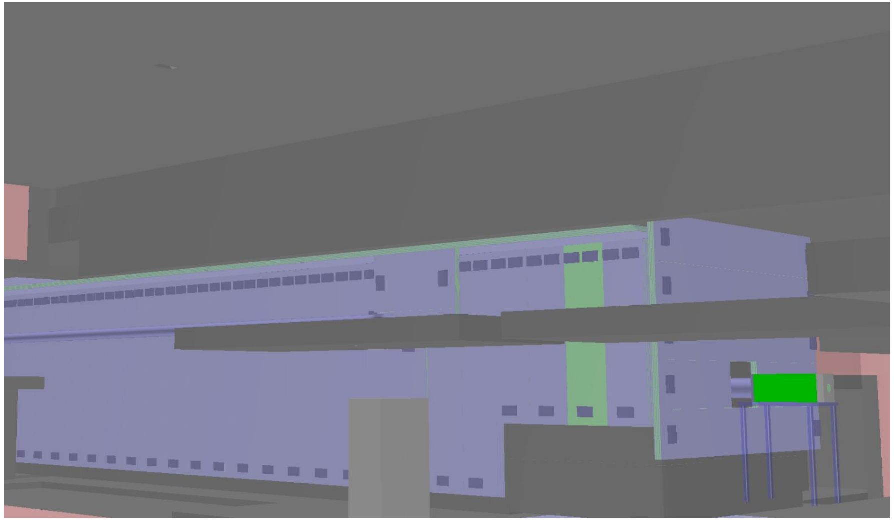

Current Geometry: 2 Ge detectors (should be one HPGe and one LaBr) with an aluminium layer without the cathode hole.

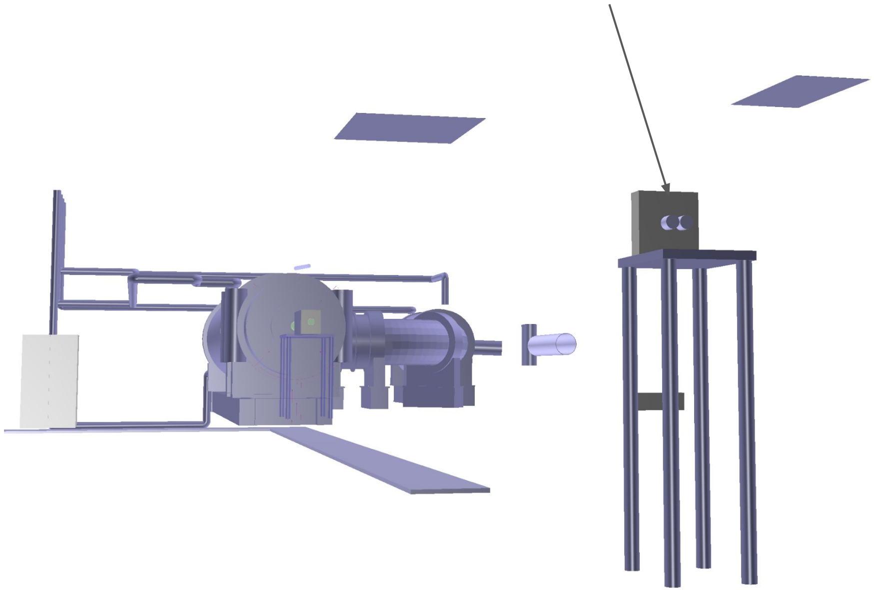

Testing the Geometry and outputs.

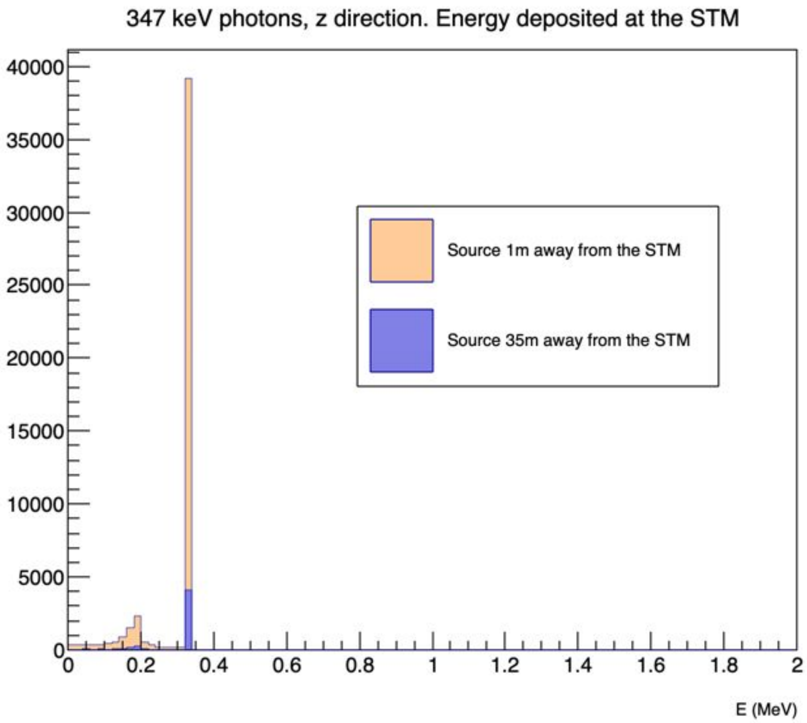

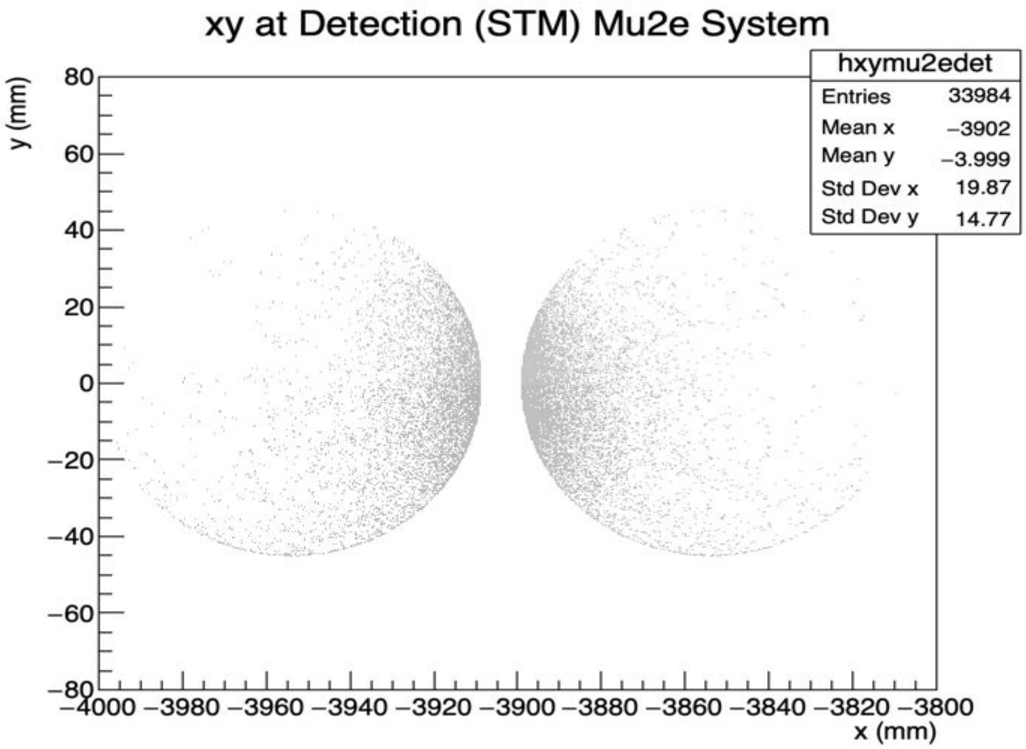

The number of photons depositing all its energy in the photopeak is reduced a factor of ~10 with distance.

Attenuation due to Solid Angle from Stopping Target to STM.

Conclusions.

- STM DAQ for HPGe: Acquiring data, developing algorithms (MWD + Pulse Finding) and analysing data.

- Literature review and Geant4 simulation to define the theoretical HPGe resolution and efficiency due to the fluctuation in the number electron hole pairs created.

- Work in progress: ART STM simulation to fully reproduce the conditions in the experiment and implementation of the zero suppression algorithm in the FPGA.
- Attended Courses: C++/STL Fermilab course and relevant Mu2e meetings: STM DAQ, STM General, Mu2e Weekly.

Back-up…

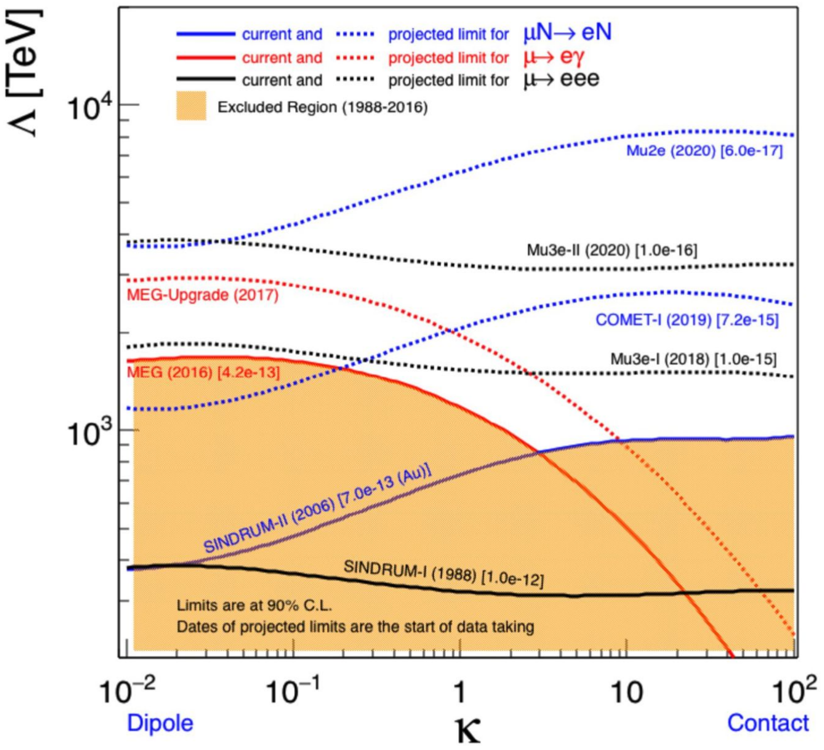
Λ [TeV]
current and projected limit for μN→ eN
current and projected limit for μ→ eγ
current and projected limit for μ→ eee
Excluded Region (1988-2016)
Mu2e (2020) [6.0e-17]
Mu3e-II (2020) [1.0e-16]
MEG-Upgrade (2017)
COMET-I (2019) [7.2e-15]
Mu3e-I (2018) [1.0e-15]
MEG (2016) [4.2e-13]
SINDRUM-II (2006) [7.0e-13 (Au)]
SINDRUM-I (1988) [1.0e-12]
Limits are at 90% C.L.
Dates of projected limits are the start of data taking
Dipole
κ
Contact

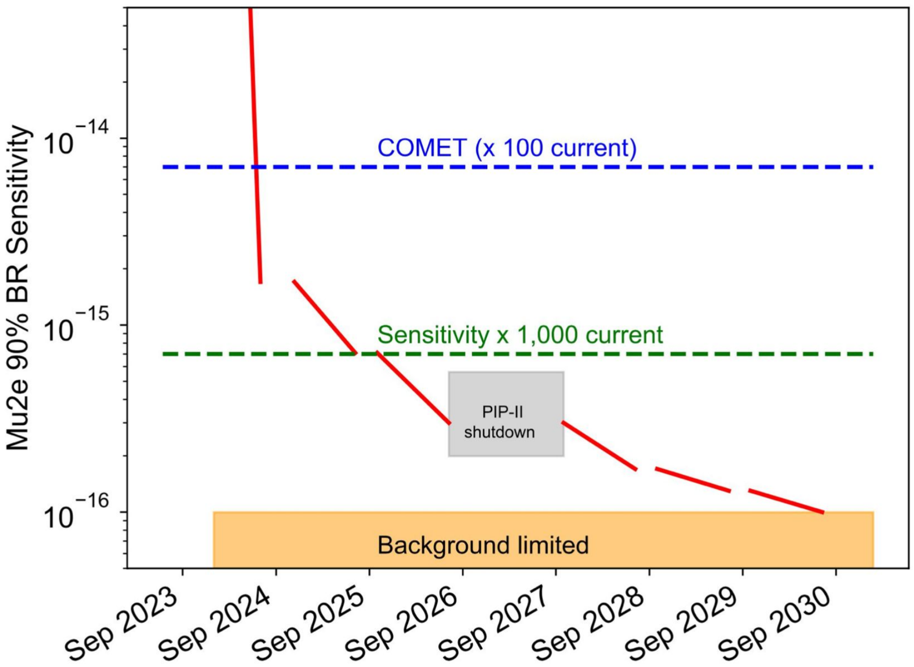
Mu2e 90% BR Sensitivity
COMET (x 100 current)
Sensitivity x 1,000 current
PIP-II shutdown
Background limited
Sep 2023
Sep 2024
Sep 2025
Sep 2026
Sep 2027
Sep 2028
Sep 2029
Sep 2030

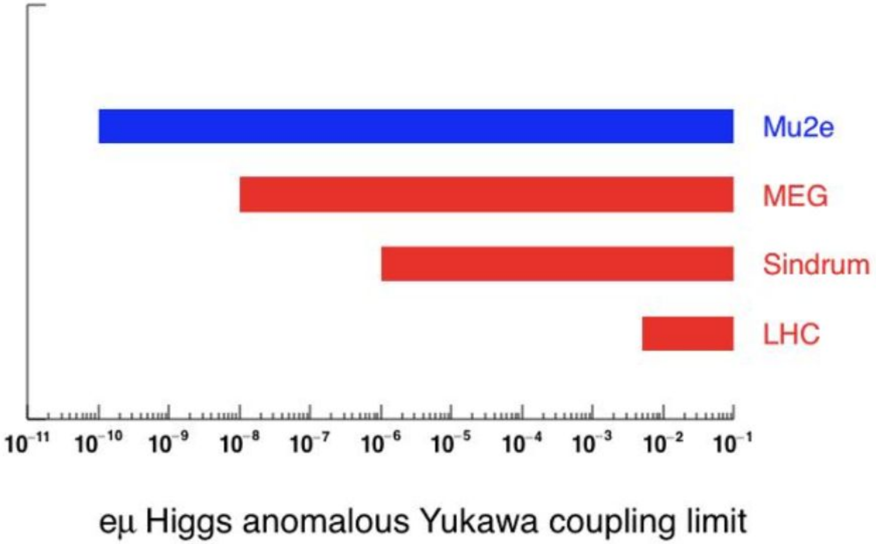
Mu2e
MEG
Sindrum
LHC
10^-11 10^-10 10^-9 10^-8 10^-7 10^-6 10^-5 10^-4 10^-3 10^-2 10^-1
eμ Higgs anomalous Yukawa coupling limit

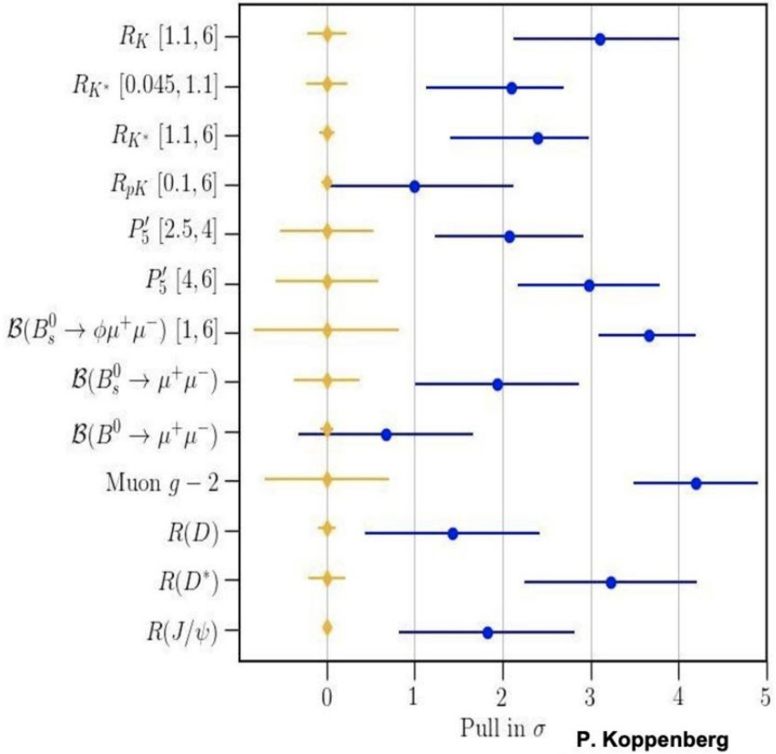
R_K [1.1, 6]
R_{K^*} [0.045, 1.1]
R_{K^*} [1.1, 6]
R_{pK} [0.1, 6]
P_5' [2.5, 4]
P_5' [4, 6]
$\mathcal{B}(B_s^0 \to \phi\mu^+\mu^-)$ [1, 6]
$\mathcal{B}(B_s^0 \to \mu^+\mu^-)$
$\mathcal{B}(B^0 \to \mu^+\mu^-)$
Muon $g-2$
$R(D)$
$R(D^*)$
$R(J/\psi)$
0 1 2 3 4 5
Pull in σ
P. Koppenberg

Effective Lagrangian, NP Model.

$$\mathcal{L}_{CLFV} = \frac{m_\mu}{(1+\kappa)\Lambda^2}\overline{\mu}_R \sigma_{\mu\nu} e_L F^{\mu\nu} + \frac{\kappa}{(1+k)\Lambda^2}\overline{\mu}_L \gamma_\mu e_L \left(\sum_{q=u,d} \overline{q}_L \gamma^\mu q_L\right)$$

Dipole Term

κ<<1

Contact Term

κ>>1

In the SM extended by (sterile) massive neutrinos, the ratio for the nuclear assisted μ − e conversion:

At lowest order, the flavour violating μ−e transition originates from one-loop diagrams involving neutrinos (active and sterile)

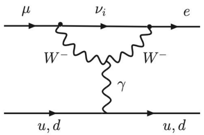

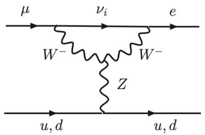

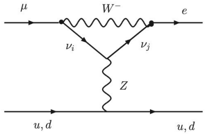

$$\mathcal{L}_{\text{eff}}^{\mu-e} = \frac{g_w^2}{2\,(4\pi)^2\,M_W^2}\left(\frac{\sqrt{4\pi\alpha}}{2}\, m_\mu\, G_\gamma^{\mu e}\, \bar{e}\,\sigma_{\lambda\rho}\,\mu_R\, F^{\lambda\rho} + g_w^2 \sum_{q=u,d} \tilde{F}_q^{\mu e}\, \bar{e}\,\gamma_\rho\,\mu_L\,\bar{q}\,\gamma^\rho\, q\right) + \text{H.c.}$$

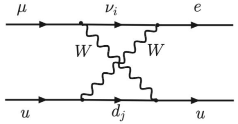

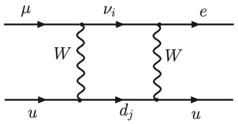

"3+1" model and cLFV processes.

- Cosmological bounds would have typically disfavoured regions in parameter space for which $m_4 < 0.1$ GeV, and hence are not visible in Fig. 3.)
- 3+1 model - can easily account for sizable contributions to CR(μ −> e, Al).
- EW scale ($m_4 \sim 10^2$ GeV), the leading contributions arise from Z-penguin diagrams; below the EW scale, box diagrams become increasingly important, and dominate the total width below a few GeV.

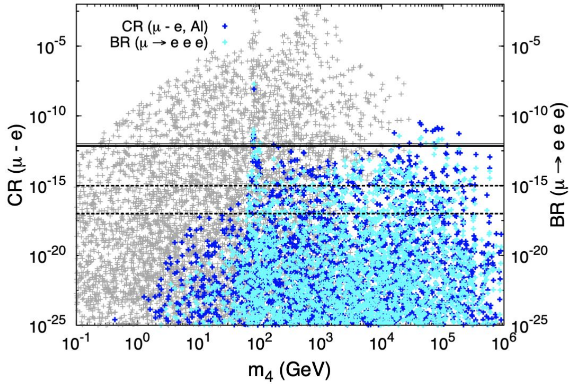

Figure 3: Effective "3+1 model": CR($\mu - e$, Al) and BR($\mu \to eee$) as a function of the mass of the mostly sterile state m_4. The former is displayed in dark blue (left axis), while the latter is depicted in cyan (right axis). Grey points correspond to the violation of at least one experimental bound (other than those arising from CR($\mu - e$, Au) and BR($\mu \to eee$)). A thick (thin) solid horizontal line denotes the current experimental bound on the CR($\mu - e$, Au) [4] ($\mu \to eee$ decays [85]), while dashed lines correspond to future sensitivities to CR($\mu - e$, N) [7,8], see Tables 2 and 3.

Impact of sterile neutrinos on nuclear-assisted cLFV processes

Cross Section: photon-matter.

$$\sigma = \sigma_{PE} + \sigma_{COH} + \sigma_{INCOH} + \sigma_{PAIR} + \sigma_{TRIP} + \sigma_{ph.n}$$

- σ_{PE} is the atomic photoeffect cross section.
- σ_{COH} is the Rayleigh scattering (coherent scattering).
- σ_{INCOH} is the Compton scattering (incoherent scattering).
- σ_{PAIR} is the cross sections for electron-positron pair production in the field of the atomic nucleus.
- σ_{TRIP} is the cross sections for electron-electron-positron (triplet) production in the field of the atomic electrons.
- $\sigma_{ph.n}$ is the photonuclear cross section.

Stopped/Captured muons.

$$BR_{Mu2e}(\mu^- \to e^-) = \frac{\Gamma(\mu^- +^{27}_{13} Al \to \mu^- +^{27}_{13} Al)}{\Gamma(\mu^- +^{27}_{13} Al \to \mu^- +^{27}_{12} Mg + \nu_\mu)} < 2.87 \cdot 10^{-17}$$

Ordinary muon capture on the nucleus

- Capture rate for Al is well-known from literature: 60.9% of stops.
- Stop rate:

- 80% of stops emit 347 keV X-Rays 2p-1s (1s orbit lifetime= 864 ns).
- 31% of stops/ 51% of captures emit 1809 keV gammas.

$$\mu^- +^{27}_{13} Al \to \nu_\mu +^{26}_{12} Mg^* + n$$

$$Mg^* \to {}^{26}_{12}Mg + \gamma$$

- 5.7% of stops/ 9.2% of captures emit 844 keV gammas.

$$\mu^- +^{27}_{13} Al \to \nu_\mu +^{27}_{12} Mg \xrightarrow{\beta^- \text{ (9 min)}} {}^{27}_{13}Al + e^- + \bar{\nu}_e + \gamma$$

Backgrounds.

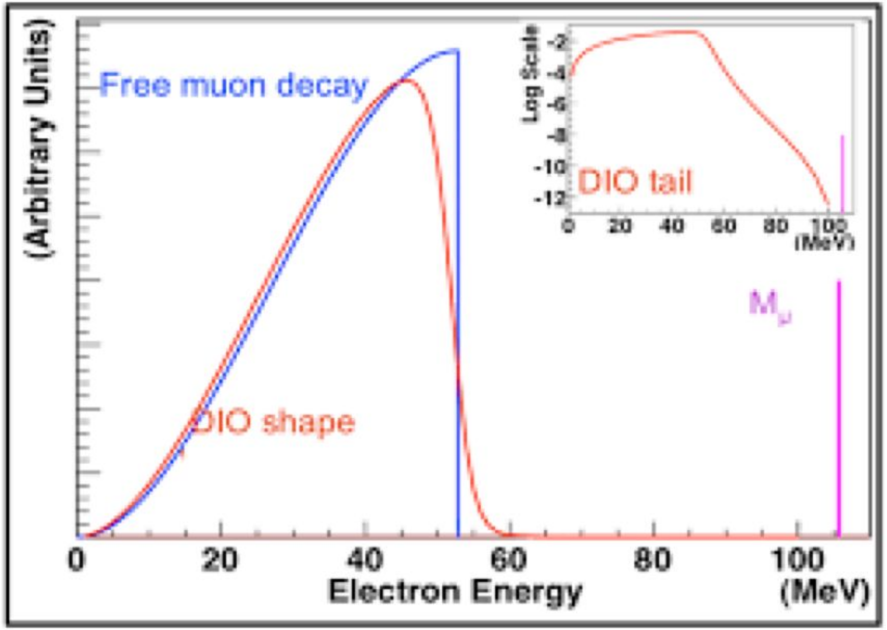

- Muon decay in orbit (DIO)
- Radiative muon capture (RMC)
- Cosmic Rays
- Radiative pion capture (RPC)

Why Aluminium?.

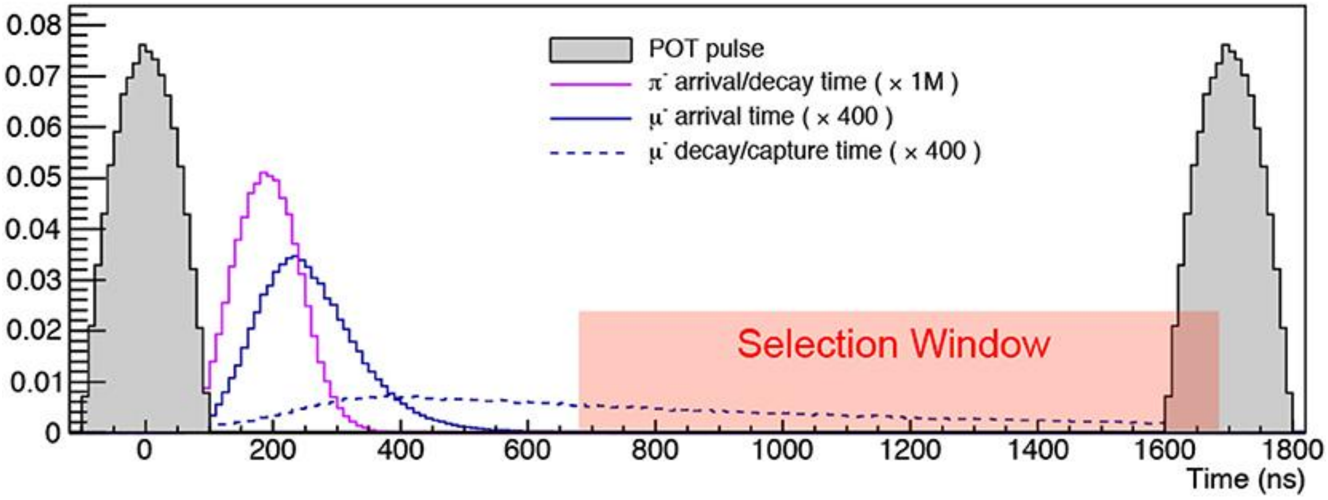

Al that stops muons will then produce bremsstrahlung photons at a rate: 51 MHz/cm^2 with a mean energy of 1.4 MeV. Many of these photons are above pair production threshold and can cause radiation damage in the STM.

The detector needs to be far from the stopping target reducing the rate by ~ 1/r^2 (r distance stopping target-STM)

Life time of a muonic atom decreases with Z:

- $_{79}$Au (τ= 74 ns): The decays occur mostly during the time pions are still arriving (physics backgrounds are high)
- $_{13}$Al (τ= 864 ns): The decays in aluminium are well separated from the flash (after 100 ns)
- $_{22}$Ti (τ= 328 ns): Also a good choice

Since the beam pulse is 250 ns wide, too many of the muons would be captured and decay within the beam flash

Momentum selection: Transport solenoid.

- “S shape”: removes neutral particles to enter the detector solenoid (unaffected by B and do not travel the S-shape)

- Particles with large momentum hit the wall of the solenoid and are not transmitted:

  $r = p_{\perp}/(0.3B)$

- μ^- and μ^+ drift vertically in opposite directions. A central collimator covering half the aperture, blocks the μ^+ and transmits the μ^-

- The second half of the S-shaped transport solenoid brings the beam back to the nominal axis and provides additional length for pions to decay, suppressing the RPC background